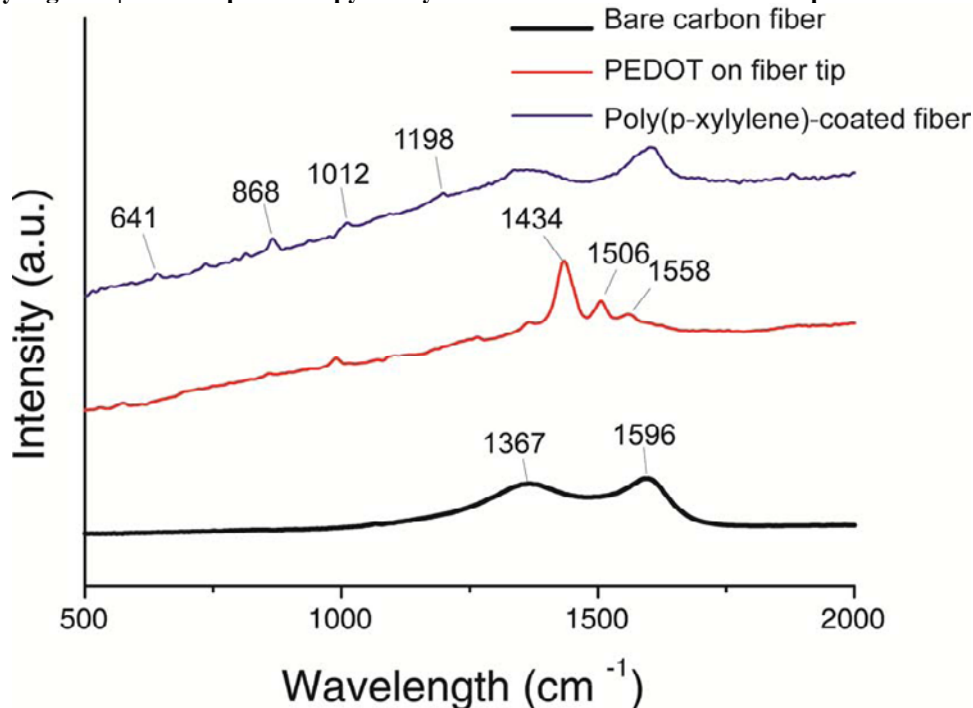


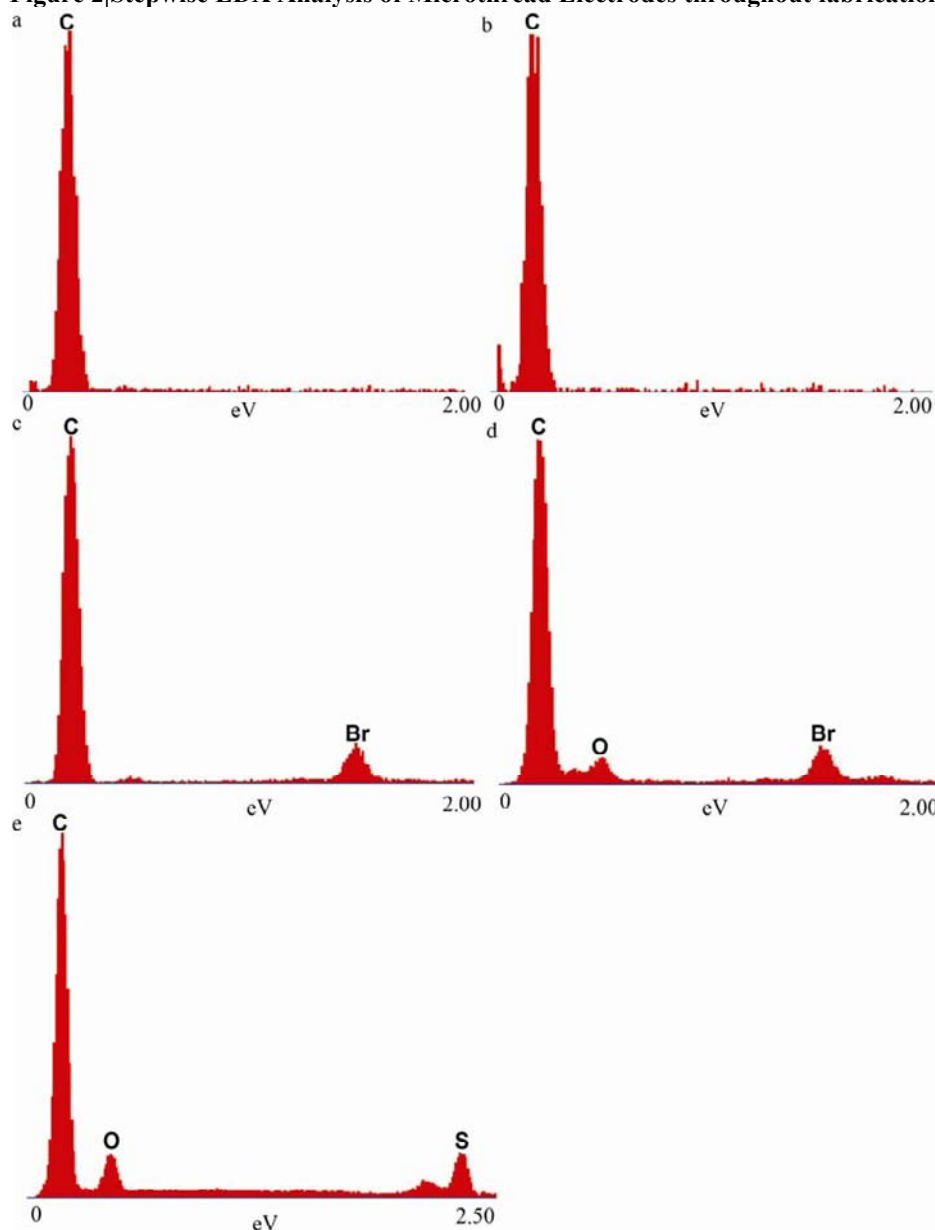
# **Ultrasmall implantable composite microelectrodes with bioactive surfaces for chronic neural interfaces**

Supplementary Figure 1 | Raman Spectroscopy Analysis of Microthread Electrode components



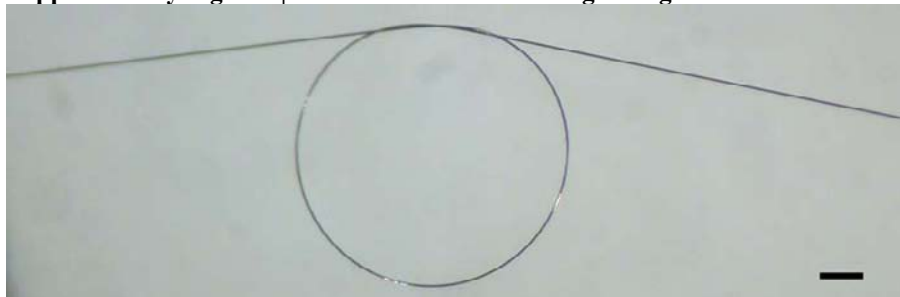
Raman Spectroscopy of bare carbon fibers (black), PEDOT recording tip (red), and poly(p-xylylene) coating (blue). Characteristic bands are labeled with their respective wavenumbers.

In order to validate each of our fabrication processes, (Fig. 1) surface materials after each step were characterized using Raman Spectroscopy (Supplementary Figure 1). Characteristic peaks of carbon fiber, parylene-N, and PEDOT were labeled with their respective wavenumbers. This demonstrates that the parylene insulation was present along the sides of the carbon fiber surface. Also, PEDOT was detected at the tip of the device, but not along the insulated sides of the microthread electrode.

**Supplementary Figure 2|Stepwise EDX Analysis of Microthread Electrodes throughout fabrication**

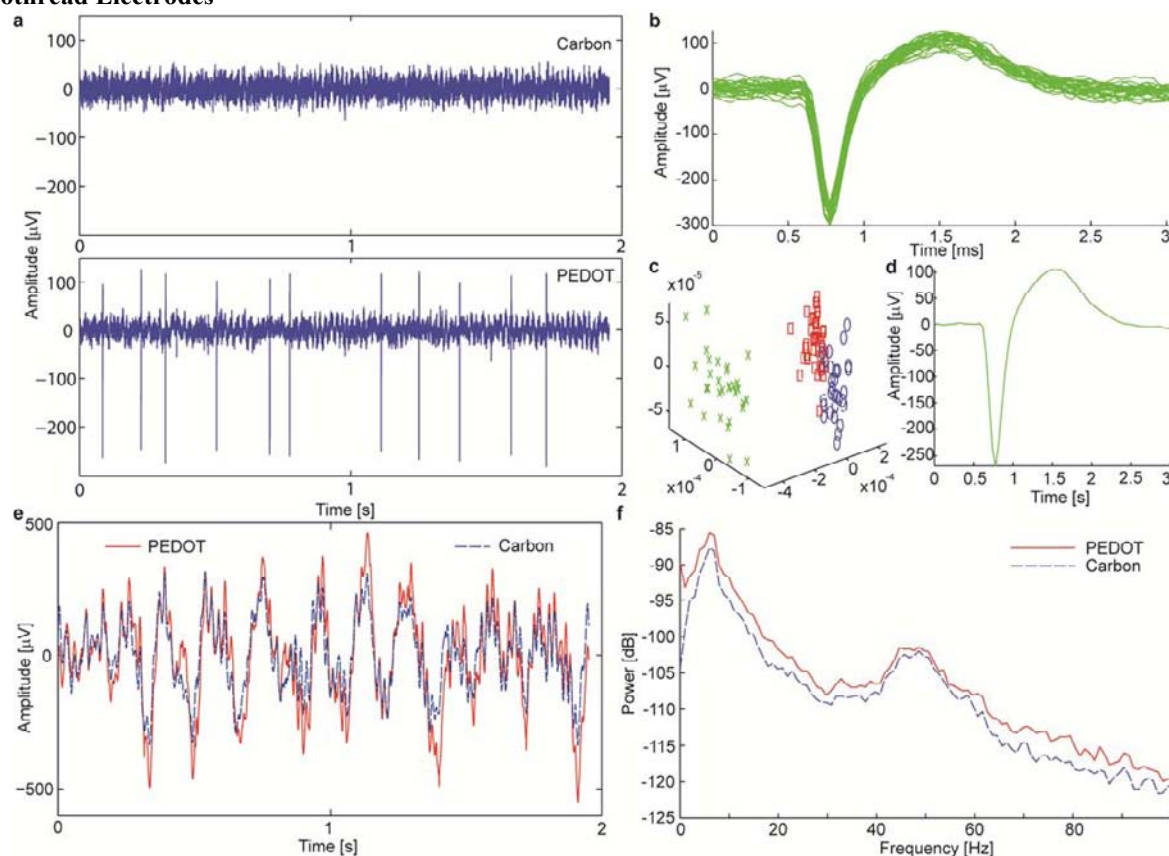
EDX data of MTE component. a, Carbon fiber, b, Poly(p-xylylene), c, Poly[(p-xylylene-4-methyl-2-bromoisobutyrate)-co-(p-xylylene)]. d, PEGMA. e, PEDOT.

The poly[(p-xylylene-4-methyl-2-bromoisobutyrate)-co-(p-xylylene)] and PEGMA coatings were not detectable using Raman Spectroscopy, perhaps due to low activity of their Raman scattering frequencies. Therefore, EDX was also used to characterize the surface material after each fabrication step (Supplementary Figure 2). Carbon fiber and parylene-N are both made of only carbon elements, so they were not discernable using EDX (Supplementary Figure 2a, 2b). The bromine element could be detected after the 50 nm coating with poly[(p-xylylene-4-methyl-2-bromoisobutyrate)-co-(p-xylylene)] (Supplementary Figure 2c). An increase in oxygen was detected as expected after the PEGMA coating (Supplementary Figure 2d). Sulfur was detected in PEDOT at the tip of the assembled Microthread Electrode (Supplementary Figure 2e). This suggests that each component of the fabrication is assembled into the Microthread Electrode.

**Supplementary Figure 3 | Demonstration of bending strength of Microthread Electrode**

MTE can withstand substantial bending into, for instance, a loop-knot without any fracturing. Scale bare indicates 100 microns.

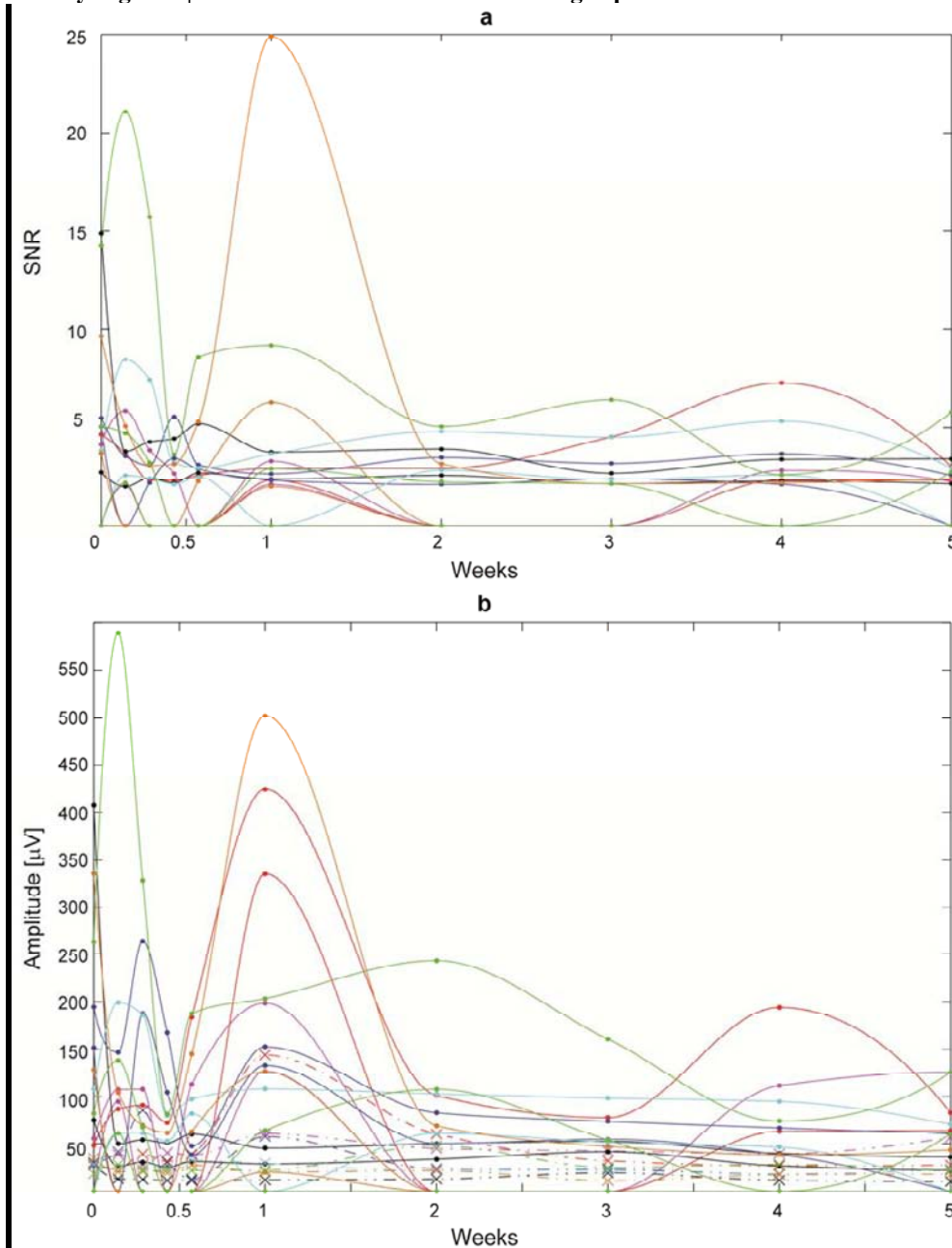
### Supplementary Figure 4 | *In vivo* single unit recording capabilities of active ester grafted PEGMA coated Microthread Electrodes



**a**, Two-fiber Microthread Array implanted 1.6 mm deep into cortex. **b**, Representative example of two seconds of high-speed recordings taken simultaneously on the same array. Recordings on the carbon site channel show no discernible single units with a noise floor of  $21.9 \mu\text{V}$  (top), while recordings taken on the channel with the PEDOT site shows a signal-to-noise ratio of 19.3 and peak-to-peak noise of  $19.4 \mu\text{V}$  (bottom). **c**, Piled single unit neural recordings over three minutes from a parylene-N coated PEDOT MTE. **d**, Results from principal component analysis showing three distinct clusters. **e**, Mean waveform for the largest unit spike. **f**, Raw local field potential (LFP) simultaneously recorded across both channels. The PEDOT site channel recorded a noise floor of  $254 \mu\text{V}$  (solid red), while the carbon site channel recorded a noise floor of  $283 \mu\text{V}$  (dash blue). **g**, Power density spectra across the LFP range showing that for the LFP range both recording materials are similar.

An alternative PEGMA grafting technique to ATRP was explored using an active ester functionalized parylene, poly(p-xylylene carboxylic acid pentafluorophenolester-co-p-xylylene)<sup>1</sup>. Acutely, this alternative coating technique demonstrated no noticeable difference in electrophysiological recording performance compared to ATRP PEGMA MTEs (Supplementary Figure 3).

Supplementary Figure 5 | Individual chronic *in vivo* recording capabilities of Microthread Electrodes

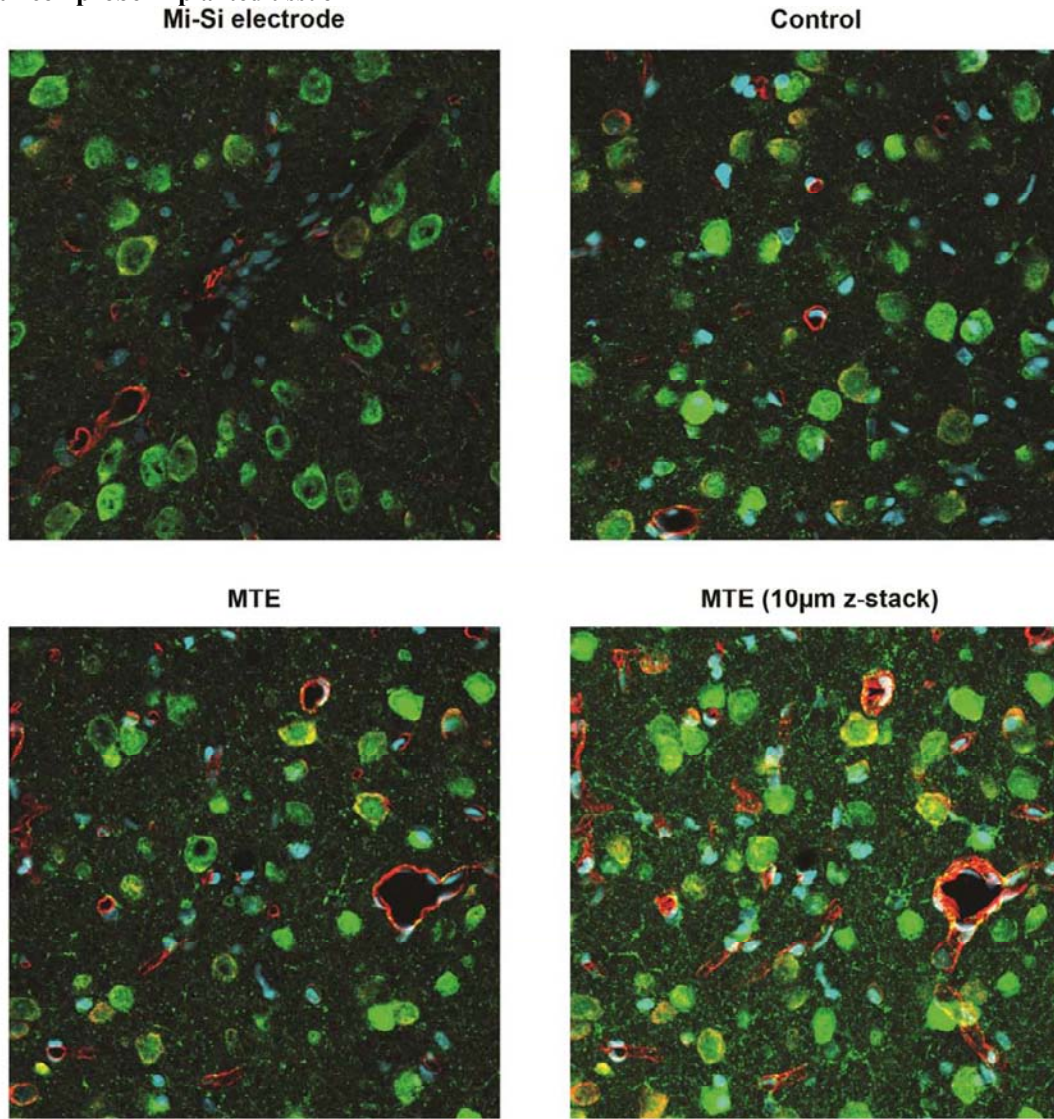


**a**, SNR of discernable single units detected on each electrode as indicated by color (red, orange, green, blue, cyan, purple, black). **b**, Amplitude of discernable single unit detected on each electrode (solid), and the mean noise floor of each electrode (dashed) as indicated by color, respectively. Measurements were taken the first five days and once a week subsequently.

Electrode performance was tracked over time (Fig. 5, Supplementary Figure 4). SNR of distinguishable units was tracked over time on each electrode (Supplemental Figure 4b). While there is one particular electrode that had a very good signal-to-noise ratio at one week, most other electrodes showed a similar trend of exhibiting a peak in SNR around one week. The signal amplitude of each distinguishable unit and the noise floor were examined to determine if the fluctuations in SNR were due to fluctuations in the signal or noise (Supplementary Figure 4b). The major fluctuation in the first 1-2 weeks post-implant appears to be largely influenced by changes in signal amplitude, as the noise floor appears to be fairly stable. This suggests the neural sources are moving relative to the electrode, perhaps through inflammation moving them, or damage causing close ones to fall silent.



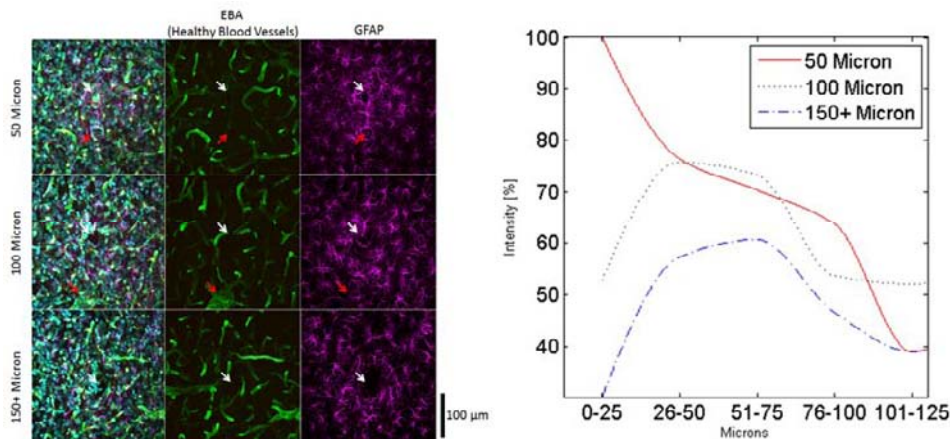
**Supplementary Figure 6 | Chronic histological comparison of neuronal distributions between Microthread and Michigan silicon probe implanted tissue**



Two week implanted tissue stained with NeuN (green) and laminin (red), and counter-stained with Hoescht (blue) imaged with a confocal microscope. Optical sections are  $\sim 1$  micron thick. Scale bar indicates 10 microns.

Neuronal proximity to the electrode probe track was examined. Laminin which labels the BBB was used to label large penetrating vasculature to distinguish it from the Microthread probe track. An increase in glial cell bodies can be seen adjacent to the silicon probe track (Fig. 6, Supplementary Figure 5). Neuronal cell distribution can also be seen to decrease immediately adjacent to the silicon probe recording site where the Hoescht labeled cells have accumulated. In contrast, five NeuN labeled cells can be identified within 20 microns of the Microthread probe track. This data supplements Fig. 6 in suggesting that the Microthread electrode can elicit a lesser tissue response compared to traditional silicon devices.

**Supplementary Figure 7|Chronic histological comparison of GFAP activation with respect to major vasculature proximity**



Lastly we show how astroglial reactivity to the probe with respect to implantation proximity to major vasculature (>25 micron diameters). This suggests that microstructures in the brain may be associated with chronic performance. Decreasing the probe's profile may improve the probability of avoiding key microstructures during insertion.

Here, we have presented a more comprehensive material characterization of the Microthread electrode, demonstrated an alternative fabrication technique to ATRP, and presented additional detail in the chronic stability of these devices. Collectively, these findings demonstrate the identity and capabilities of these chronic microsensors.



## Supplemental Methods

### *Carbon Fiber Microthread Electrodes*

One, two, or three individual 7  $\mu\text{m}$  diameter (Cytec Thornel T650, tensile modulus = 234 GPa) carbon fibers were mounted onto a NeuroNexus A16 printed circuit board or a bare stainless steel wire using silver epoxy (WPI; Sarasota, FL) and baked at 140  $^{\circ}\text{C}$  for 10 min. An  $\sim 800$  nm thick poly(p-xylylene) insulator layer was then coated via CVD. One gram of paracyclophane was sublimed at 90–110  $^{\circ}\text{C}$  and 0.3 mbar and carried into the pyrolysis chamber by argon at a flow rate of 20 standard cubic centimeters per minute (sccm). After pyrolysis at 670  $^{\circ}\text{C}$ , the polymer was deposited on the substrate at 15  $^{\circ}\text{C}$ . The deposition rate, according to the QCM, was 0.6–1.0  $\text{\AA}/\text{s}$ . Next, the surface was functionalized with a  $\sim 50$  nm thick poly[(p-xylylene-4-methyl-2-bromoisobutyrate)-*co*-(p-xylylene)] layer via CVD. [2.2]paracyclophane-4-methyl 2-bromoisobutyrate was sublimed at 90–110  $^{\circ}\text{C}$  and 0.3 mbar and carried into the pyrolysis chamber by argon at a flow rate of 20 standard cubic centimeters per minute (sccm). After pyrolysis at 550  $^{\circ}\text{C}$ , the polymer was deposited on the substrate at 15  $^{\circ}\text{C}$  at 0.6–1.0  $\text{\AA}/\text{s}$ .

### *Atom Transfer Radical Polymerization*

Poly(ethylene glycol methacrylate) was grafted onto the poly(p-xylylene) surface by atom transfer radical polymerization (ATRP). Poly[(p-xylylene-4-methyl-2-bromoisobutyrate)-*co*-(p-xylylene)] was used as initiator for ATRP because of its functional groups<sup>2</sup>. After deposition of poly[(p-xylylene-4-methyl-2-bromoisobutyrate)-*co*-(p-xylylene)], MTEs were incubated under inert conditions with a degassed aqueous solution of oligo(ethylene glycol) methyl ether methacrylate, with CuBr/CuBr<sub>2</sub>/bpy as the catalyst. The polymerizations proceeded at room temperature for 4 hours. Surface-modified MTEs were thoroughly rinsed after the reaction.

### *Alternative to ATRP: Grafting to Functionalized Coating: Active Ester*

Poly(p-xylylene carboxylic acid pentafluorophenolester-*co*-p-xylylene) is a polymer with an active ester group which can readily react with a primary amine<sup>1</sup>. After chemical vapor deposition of poly(p-xylylene carboxylic acid pentafluorophenolester-*co*-p-xylylene), MTEs were incubated in 10mM mPEG-NH<sub>2</sub> (MW 10,000) phosphate buffer saline (PBS) solution for 8 hours, followed by thorough rinses in PBS.

### *Recording Site*

Poly(p-xylylene)-coated and PEGMA-grafted carbon fibers were cut to a length of 0.3–0.5 cm. For PEDOT deposition, monomer 3,4-ethylenedioxythiophene (EDOT) (Bayer, Germany) was electrochemically polymerized and deposited onto the surface of the electrode sites together with the anions in the solution. Specifically, PEDOT/PSS was electropolymerized from a 0.1 M poly(sodium-p-styrenesulfonate) (PSS) (Acros Organics, Morris Plains, NJ) aqueous solution with an EDOT concentration of 0.01 M under galvanostatic conditions. In galvanostatic mode, the current was held at 100 pA.

### *Electrical Characterization*

EIS and CV measurements were made using an Autolab potentiostat PGSTAT12 (Eco Chemie, Utrecht, The Netherlands) with associated frequency response analyzer and general purpose electrochemical system software (Metrohm, Westbury, NY), respectively. To obtain EIS and CV measurements, each probe was submerged in a PBS solution of 137 mM sodium chloride, 2.7 mM potassium chloride, and 11.9 mM phosphate buffer with a stainless steel rod serving as the counter electrode and a standard Ag|AgCl probe as the reference. Impedance measurements were taken between 10 Hz and 31 kHz at 25 mV<sub>rms</sub>. CV values were obtained by cycling three times from 0.8 V to -0.6 V at a sweep rate of 1 V/s and averaging the last two cycles. Charge storage capacity (CSC) of each site was calculated from the full area under the CV curve, scaled by the inverse of the scan rate. After implantation, a distant stainless steel (316-SS grade) bone screw was used as the reference and counter electrode.

### *Protein Adsorption*

Poly(p-xylylene)-coated and PEGMA-grafted devices were incubated in FITC-albumin in 2 mg/ml PBS solution for 60 min, then washed in PBS for 30 min. Confocal images were taken with an SP2 confocal laser scanning microscope (Leica, Buffalo Grove, IL). Immediately after, FITC-albumin was imaged with an Ar/ArKr laser at 488 nm. Biofouling was calculated by measuring the intensity of the probe after adsorption and normalizing it against the background intensity.

*Characterization of Mechanical Properties*

The stiffness ( $k$ ) of a MTE calculated from;

$$k = \frac{AE}{l} \tag{1}$$

where the cross-sectional area ( $A$ ), elastic modulus ( $E$ ) and length implanted into the cortex ( $l$ ). The cantilever beam spring constant ( $k_c$ ) can be calculated from;

$$k_{c(\text{planar})} = \frac{3wct^3}{4l^3} \tag{2}$$

$$k_{c(\text{cylindrical})} = \frac{3\pi E(d_o^4 - d_i^4)}{64l^3} \tag{3}$$

where  $t$  is the thickness,  $w$  is width,  $d_o$  is outer diameter, and  $d_i$  is inner diameter. Compliance was calculated as the inverse of  $k$  and  $k_c$ . Insertion force was calculated from the critical buckling force  $F_{crit}$ ;

$$F_{crit} = \frac{n^2 E I (\pi - \alpha)^2}{4l} \tag{4}$$

for a cylinder with one fixed end and a hinged end when  $l$  was too long to insert (5mm).

*SEM Imaging*

SEM imaging was carried out on a FEI Quanta 200 3D Focused Ion Beam Workstation (FEI, Hillsboro, OR). Samples were sputter coated with gold prior to imaging.

*Microscopic Raman Spectroscopy*

The carbon nanotube samples were analyzed using a Bruker SENTERRA Raman system (Bruker Optik GmbH, Ettlingen, Germany) based on an Olympus BX 51 microscope (Olympus Corp., Tokyo, Japan), and an Olympus UIS-2 LMPlanFL N 100x/0.80 objective (Olympus Corp. Tokyo, Japan) with 2  $\mu$ m resolution used for the lateral and axial directions. The equipped 532 nm laser was chosen for the measurements of the sample surfaces. In order to avoid thermal decomposition of the sample, the laser power was attenuated to 2mW for the analysis. The spectra were recorded in the region from 100 to 4000  $\text{cm}^{-1}$  for each sample.

*EDX Analysis*

Energy-dispersive X-ray spectroscopy (EDX) is a technique for elemental analysis of a sample. This technique is based on the fundamental principle that each element has a distinct atomic structure, which emits a unique characteristic X-ray to be analyzed. It relies on analyzing X-rays emitted by the sample upon hitting it with charged particles. The inner shell electrons of the atoms in ground state could be ejected by the high energy particles. The outer shell higher energy electrons would replace the hole from the ejected electron. An X-ray would be emitted during this process due to the difference in the energy between the inner and outer electrons. The number and energy of the X-rays emitted from a sample can be measured by an energy-dispersive spectrometer, and this allows the elemental composition of the sample to be measured.

*Surgery*

The microthread probes were manually inserted into rat cerebral cortex to validate the insertion technique in a typical experimental preparation. Adult male Sprague-Dawley rats (Charles River Laboratories, Wilmington, MA) weighing 300-350 g were prepared for cortical implants using previously established methods<sup>3</sup>. The animal was anesthetized with a mixture of 50 mg/mL ketamine and 5 mg/mL xylazine administered intraperitoneally with an initial dosage of 0.125 mL/100 g of body weight and regular updates of ketamine. The depth of anesthesia was observed by monitoring heart rate and blood oxygen saturation. The animal was placed into a stereotaxic frame and a 2 mm by 2 mm craniotomy was made over the motor cortex. The dura was incised and resected. Sterile saline was used to keep the brain surface moist throughout the procedure. A stereotaxic frame mounted micromanipulator guided insertions of the MTE 2 mm into the cortex. Due to the stiffness of the carbon fiber, a 2.5-5 mm long fiber did not need additional assistance penetrating the

cortex when aligned perpendicularly to the cortical surface. For chronic implants, a bone-screw grounded the electrode connected over parietal cortex using a stainless steel ground wire. Surgical closure was achieved with a combination of silicone (World Precision Instruments, Sarasota, FL), and Cerebond adhesive (MyNeuroLab, St. Louis, MO). For chronic histology, a 5 mm Michigan Silicon Electrode (NeuroNexus Technologies, Ann Arbor, MI) was inserted 500  $\mu\text{m}$  away from the MTE. Both probes were tethered to the skull using silicone and Cerebond adhesives. All procedures complied with the United States Department of Agriculture guidelines for the care and use of laboratory animals and were approved by the University of Michigan Committee on Use and Care of Animals.

#### *Vasculature and BBB Disruption: Acute Histological Imaging*

A 5 mm Michigan silicon electrode was inserted into the cortex at least 49  $\mu\text{m}$  away from all surface vessels<sup>24</sup>. Immediately after, a MTE was inserted into the cortex at least 1 mm away from the silicon electrode. 2 % Evans Blue (EB) at a dose of 2 mL/kg of body weight was injected intravenously into the tail vein at a rate of 0.45 mL/min. Brains were immediately fixed with a transcardial perfusion with 100 mL of PBS followed by 250 mL of 4 % paraformaldehyde solution in pH 7.4 phosphate buffer, and then fixed in the same solution for another 24 hrs. Tissue was then rinsed with PBS twice for 15 min to remove any excess paraformaldehyde. All procedures complied with the United States Department of Agriculture guidelines for the care and use of laboratory animals and were approved by the University of Michigan Committee on Use and Care of Animals.

The tissue sample was removed from the fixative and placed in 15 % sucrose w/v in 1X PBS until the brain sank to the bottom of the solution. The sample was then transferred to a 30 % sucrose solution until sunk. For 1-3 hr, the sample soaked in 30% sucrose:OCT embedding media (2:1) solution. A cryomold was filled with 20% sucrose:OCT embedding media (2:1) solution and the block of tissue placed within the mold. A weigh boat was filled with 2-methylbutane and placed in dry ice for 15 min. After 15 min, the cryomold was placed in the weigh boat with the 2-methylbutane. Care was taken to ensure that the solution did not flood the inside of the mold. The sample was then allowed to slowly freeze. Upon complete freezing, sample was stored in a -80 °C freezer.

Samples were “thawed” to -20 °C at least 1 hour prior to sectioning. Each brain was then sliced on a cryostat into sections 30  $\mu\text{m}$  thick and then, without further staining, placed on slides and coverslipped with ProLong Gold (Invitrogen, Carlsbad, CA) for microscopic examination.

The sections were imaged under an Olympus BX51 fluorescence microscope (Olympus Corp., Tokyo, Japan) for staining intensity. EB absorbs at 470 nm & 540 nm and emits at 680 nm. Dye indicates neural vasculature and locations in the brain where the microelectrode disrupted the vasculature and compromised the BBB.

#### *In vivo Neural Recordings*

For all animals in this study, electrophysiological data were acquired using a TDT RX5 Pentusa recording system (Tucker-Davis Technologies, Alachua, FL). These neuronal signals were acquired through a head-stage buffer amplifier to avoid signal loss in data transmission. Signals were sequentially filtered by an anti-aliasing filter in the preamplifier, digitized at a ~ 25-kHz sampling rate, and digitally band-pass filtered from 2 to 5000 Hz. Wideband signals were acquired to capture both spiking and LFP activity. Signals were continuously recorded in segments ranging from 30 seconds to > 10 minutes in duration.

Neural recording segments were analyzed offline to determine the number of neurons recorded, noise levels, and signal amplitudes using custom automated MATLAB (Mathworks Inc., MA) software, as described elsewhere<sup>7</sup>. As an overview, the wide-band recordings were filtered in software to isolate the spike data (300–5000 Hz) from the LFP data (1–100 Hz). The LFP power spectral density plots were created using a Hamming window for smoothing with a 32768-point fast Fourier transform (FFT). Low frequency activity in the range typically observed for LFPs is presented. To identify individual units, the threshold for the high-frequency data was established by using a window set at 3.5 standard deviations below the mean of the data. A 3 msec waveform was extracted from the data stream at each threshold crossing. To group isolated waveforms to a single neuronal unit, principal component analysis was then completed, and the resultant components were separated into individual clusters by using Fuzzy C-means clustering. Units with sufficiently clustered principal components were plotted, and the signal-to noise ratio was calculated as the peak-to-peak amplitude of the mean waveform of the cluster divided by two times the standard deviation of the remaining data stream after all waveforms had been removed. If a single unit was not detected, the SNR and amplitude were considered 0 and 0  $\mu\text{V}$

respectively, unless otherwise stated. Recordings from the control group of chronically implanted Silicon Electrodes from a previous study<sup>4</sup> were re-analyzed using these parameters.

#### *Chronic Immunohistochemistry: BBB, Astrocytes, Microglia, Nuclei*

Rats were perfusion-fixed with 4% paraformaldehyde two weeks after implant. Brains were then dissected with devices in place and block-fixed for 24 hrs at 4 °C. Devices were removed; the brains were blocked, and 100 µm vibratome tissue slices were cut in a direction perpendicular to the long axis of the inserted device. Sections were then treated with 5 mg/mL sodium borohydride in HEPES-buffered Hanks saline (HBHS) for 30 min, followed by three rinses with HBHS. In all steps involving HBHS, sodium azide (90 mg/L) was included. Tissue sections were then incubated in 0.5% (v/v) Triton X-100 in HBHS for 30 min, followed by three washes with HBHS and then blocked overnight at room temperature with 5% (w/v) goat serum. Sections were washed four times, for 30 min each, with HBHS. A multi-step immunohistochemical approach was needed due to cross reactivity seen when applying both the rat anti-GFAP primary and the mouse anti-blood brain barrier (EBA) primary simultaneously. Our experience with the GFAP antibody indicates that the EBA primary and subsequent secondary needs to be applied first, followed by the GFAP primary and other primary antibodies. This method yields two completely separated channels for GFAP and EBA. The method is as follows: tissue was incubated overnight at room temperature with the EBA primary antibody (1:300, Covance #SMI-71R, lot #2) with 0.2% triton. After 24 hrs, the sections were washed four times for 30 min each with HBHS. Sections were then incubated in a secondary antibody with 0.2% triton (1:200; Alexa Fluor 494 goat anti-mouse secondary antibody; Invitrogen, Carlsbad, CA), overnight at room temperature. After four 30 min washes, the tissue was incubated overnight at room temperature with the GFAP primary antibody (targeting astrocytes, 1:1000, Invitrogen #13-0300, lot #686276A) and rabbit anti-Iba-1 primary antibody (targeting microglia, 1:800, Wako #019-19741, lot #STN0674) containing 0.2% triton. After 24 hrs, the sections were washed four times for 30 min each with HBHS. Sections were then incubated in a secondary antibody solution with 0.2% triton (1:200; Alexa Fluor 546 goat anti-rat, 1:200; Alexa Fluor 488 goat anti-rabbit secondary antibody; Invitrogen, Carlsbad, CA) and Hoechst 33342 (nuclei stain, 1:150, Invitrogen #H-1399, lot #46C3-4), overnight at room temperature. After the final washes (four times for 30 min each with HBHS), tissue slices were mounted on slides with coverslips using Prolong Gold mounting media. The slides remained covered (protected from light) at room temperature and allowed to clear for at least 12 hrs prior to imaging.

#### *Chronic Immunohistochemistry: Imaging and Image Processing*

Images were obtained on a Leica TCS SP5 scanning laser multiphoton confocal microscope (Leica, Buffalo Grove, IL). All images were collected using a 40x objective (1.30 NA with a zoom of 1.25 = final 50x). Individual Z slices were acquired at 0.63 µm step sizes. The nuclei channel was collected in sequence using the multiphoton. Standard TIFF files were saved and colorized using Image Pro Plus (Media Cybernetics, Bethesda, MD). Immunomarkers were quantified using fluorescent intensity as a function of distance from the implant surface using a custom MATLAB script. Probe footprint of appropriate dimensions was placed into the center of the probe track. The MATLAB script assigned each pixel in the probe track a radius of 0, and then calculated the distance of each other pixel to the nearest probe surface. Average intensities of 20 micron bins of each image were calculated for pixels with distance,  $d$ , values  $0 < d \leq 20$ ,  $20 < d \leq 40$ , etc.

#### *Chronic Immunohistochemistry: Neuron, BBB, Nuclei*

Rats were perfusion-fixed two weeks after implant with 4% paraformaldehyde. Brain tissue was explanted, postfixed overnight in 4% paraformaldehyde, and cryoembedded following sucrose protection. Each brain was then sliced on a cryostat into sections 10 µm thick and stored at -80 °C. Tissue 1 to 1.5 mm deep from the surface were randomly selected and immunostained for NeuN (targeting neurons, 1:200, AbCam #ab77315), Laminin (1:500, AbCam #ab11575), and counterstained with Hoechst 33342 (1:5000, Invitrogen #H3570). Sections were hydrated and blocked with 10% normal goat serum in PBS at room temperature for 1 hour. Samples were then incubated with primary antibodies in 0.3% Triton-X100 and 3% normal goat serum in PBS overnight in a humidified chamber at room temperature. Sections were then rinsed, incubated in the appropriate secondary antibodies (1:200 Alexa, 488, and/or 568, Invitrogen, Carlsbad, CA), counterstained with Hoechst, and coverslipped with ProLong Gold. Antibody solutions included 0.3% triton X-100 and 5% normal goat serum. Buffer was used in place of primary antibody for controls. Confocal images were collected with a Zeiss LSM510 microscope (Jena, Germany) with a C-Apochromat 40X/ 1.2 W corr objective.

**Reference**

- 1 Lahann, J., Choi, I. S., Lee, J., Jenson, K. F. & Langer, R. A new method toward microengineered surfaces based on reactive coating. *Angew Chem Int Edit* **40**, 3166-+ (2001).
- 2 Jiang, X. W., Chen, H. Y., Galvan, G., Yoshida, M. & Lahann, J. Vapor-based initiator coatings for atom transfer radical polymerization. *Adv Funct Mater* **18**, 27-35, doi:DOI 10.1002/adfm.200700789 (2008).
- 3 Ludwig, K. A., Uram, J. D., Yang, J., Martin, D. C. & Kipke, D. R. Chronic neural recordings using silicon microelectrode arrays electrochemically deposited with a poly(3,4-ethylenedioxythiophene) (PEDOT) film. *J Neural Eng* **3**, 59-70, doi:S1741-2560(06)12912-2 [pii] 10.1088/1741-2560/3/1/007 (2006).
- 4 Purcell, E. K., Thompson, D. E., Ludwig, K. A. & Kipke, D. R. Flavopiridol reduces the impedance of neural prostheses in vivo without affecting recording quality. *J Neurosci Methods* **183**, 149-157, doi:S0165-0270(09)00344-6 [pii] 10.1016/j.jneumeth.2009.06.026 (2009).